CrossMark

Real-time seam penetration identification in arc welding based on fusion of sound, voltage and spectrum signals

Zhifen Zhang · Shanben Chen

Abstract Sensor technology application is the key for intelligent welding process. Multiple sensors fusion has shown their significant advantages over single sensor which can only provide limited information. In this paper, a feature-level data fusion methodology was presented to automatically evaluate seam quality in real time for Al alloy in gas tungsten arc welding by means of online arc sound, voltage and spectrum signals. Based on the developed algorithms in time and frequency domain, multiple feature parameters were successively extracted and selected from sound and voltage signals, while spectrum distribution of argon atoms related to seam penetration were carefully analyzed before feature parameters selection. After the synchronization of heterogeneous feature parameters, the feature-level-based data fusion was conducted by establishing a classifier using support vector machine and 10-fold cross validation. The test results indicate that multisensory-based classifier has higher accuracy i.e., 96.5873 %, than single sensor-based one in term of recognizing seam defects, like under penetration and burn through from normal penetration.

Keywords Multisensory data fusion · Feature extraction · Feature selection · Penetration identification · Arc welding

Introduction

Sensor-based real-time monitoring of welding quality is the hot issue for the research of intelligent manufacturing

Z. Zhang · S. Chen (✉)
Institute of Welding Engineering, Material Science and Engineering, Shanghai Jiao Tong University, Shanghai 200240, China
e-mail: sbchen@sjtu.edu.cn

Z. Zhang
e-mail: zhangzhi@umich.edu

process. Aluminum alloy pulsed gas tungsten arc welding (GTAW) is widely used in the aerospace, automotive and other industries. During the welding process, the welding seam quality can be easily disturbed by various factors, like the changes of electrode position and heat input, etc. (Chen and Wu 2009) Off-line traditional testing of welds, both destructive and non-destructive can be costly in terms of time, material, and productivity. Hence, several on-line welding quality monitoring solutions by means of the sensing technique have been proposed to provide real-time information to control the welding process and seam quality, such as vision sensor (Wang and Li 2013; Chokkalingham et al. 2012; Zhang et al. 1993, 2012, 2013), arc sensor (Christner 1998; Li et al. 2013), acoustic emission sensor (Kannatey-Asibu Jr 2009; Sun et al. 1999; Emel and Kannatey-Asibu 1988), temperature sensor (Chen and Chin 1990) and spectrum sensor (Zhang et al. 2013; Mirapeix et al. 2006; Sun et al. 2002; Li and Zhang 2001). However, the single sensor applied in these reports can only obtain information reflecting the welding status from one point of view instead of the comprehensive information considering that the welding process is a highly nonlinear and time-varying complex process. Not to mention that the sensors may be easily disturbed by various and uncertain fluctuations, such as spatter, electromagnetism, noise, intense arc light, and so on. Multisensor information fusion technology, which can provide significant advantages over single sensor has the great potential of improving the satiability and robustness of the objective system and has been widely applied in different areas, such as robotics (Chilian et al. 2011; Smith and Singh 2006), intelligent transportation (Faouzi et al. 2011) and son on. Recently this technology has been tried and effectively applied in different welding process for different purpose, for instance, nugget size monitoring of resistance spot welding (Cullen et al. 2008; Chien and Kannatey-Asibu Jr 2002), welding

penetration condition estimation in CO2 laser welding (Sun et al. 2002; Farson and Kim 1999) and joint quality monitoring in ultrasonic welding process (Lee 2013). However, systemic research about data fusion of arc sound, voltage and spectrum signals in pulsed GTAW have been rarely reported yet.

In this paper, a novel methodology for real-time seam penetration identification of aluminum alloy in pulsed GTAW is presented based on the feature-level fusion of sound, voltage and spectrum signals. In order to simulating the various degree of seam penetration, the repeatable and controllable condition, e.g., under penetration, full penetration and burn through were artificially produced for plates butt welding experiment. The detailed experiment setup was carefully introduced in "Experimental setup" section. "Feature extraction of multi-sensor signals" section will introduce the developed algorithm of feature extraction for the three signals respectively before the thorough analysis of the relationship between these feature parameters and the seam penetration in "Synchronization of heterogeneous feature data" section. The feature-level-based data fusion frame was firmly constructed in "Feature-level data fusion based on SVM-CV section", wherein the constructed classification architecture, namely, SVM-CV was proposed and utilized to identify the status of seam penetration. Moreover, the performance of the classifier was carefully compared between single sensor and multiple sensors based on the test accuracy. The method presented here has been effectively verified upon a series of experiments and is generic in nature, hence applicable to a wide range of problems typically seen in welding quality monitoring and other manufacturing process condition monitoring.

Experimental setup

The experiments were performed on an automatic experimental system which was shown in Fig. 1. It consists of three parts: the welding system, the control and motion system and multisensory signal acquisition system. The welding system includes the TIG welding power with OTC INVERTER ELESON 500P-type, CM-271 type wire feeder, water cold tank, welding torch and 99.99 % pure Argon as the shielding gas. For the control and motion system, a host computer using VC++ multithreading application was utilized to control the welding parameter, feed speed such as speed, time and so on and drive work piece to move with multiple freedoms while the torch and the designed multisensory system remained quiescent. The signal acquisition system is composed of three parts. Firstly, the arc sound sensing system includes an omnidirectional capacitance microphone, i.e., MP201, which has the frequency response from 20 Hz to 20 kHz and was fixed with the angle of 75° over the workpiece, and the MC104 signal conditioner to filter and amplify the signal. Secondly, the voltage signal was collected by means of a hall sensor used to convert the welding current to voltage signal, and a protection circuit to isolate the high-frequency interference. Both sound and voltage signal were synchronously acquired with the sampling rate of 20 kHz by a data acquisition card in the computer. Finally, the spectral collecting system consists of a low-cost 3,648-pixel spectrometer (Ocean Optics HR4000), which ranges from 185 to 1,100 nm with the resolution of 0.2 nm, an optical fiber and an optical probe. The optical probe was fixed at a two dimensional positioning stage and approximately at 32 cm away from the electrode and has a deviation of 30° from the torch center after the careful cal-
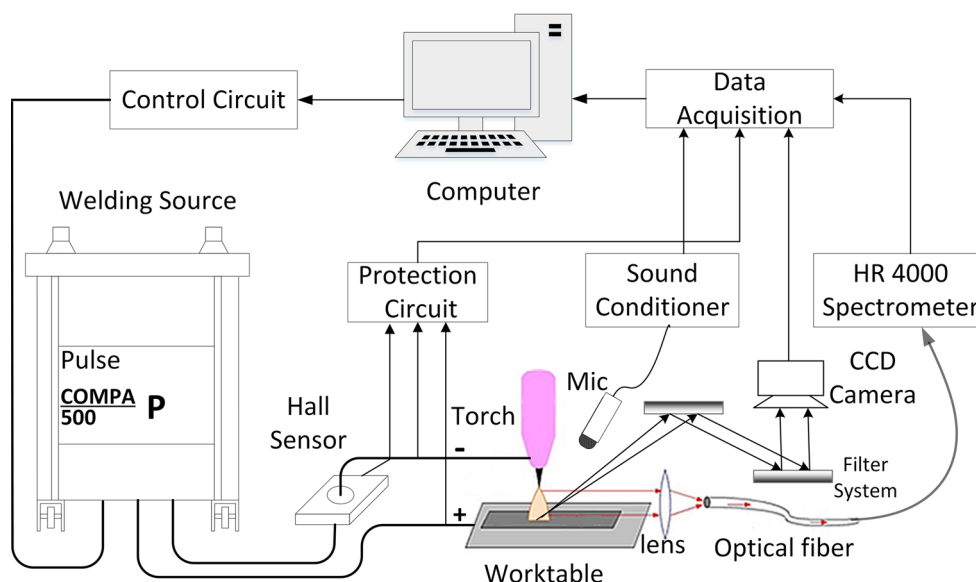

Fig. 1 Diagram of the experimental system

Table 1 Normal welding parameters

Welding parameters	Value	Welding parameters	Value
Pulse frequency (Hz)	2	Welding speed (mm/s)	3
Peak current (A)	195	Feed speed (mm/s)	10
Base current (A)	50	Electrode diameter (mm)	3.2
Pulse duty ratio (%)	50	Welding wire diameter (mm)	1.6
Ar flow (L/min)	15	Plate size (mm)	$300 \times 50 \times 4$
Material type		Al–Mg alloy (5A06)	

ibration. During the dynamic welding process, the light of welding arc is transferred into the spectrometer through the optical fiber and the final data are transferred and stored in a PC for real-time processing through USB with the sampling period of 35 ms, which gives a detection accuracy of 0.1 mm for the welded seam. In addition, the real-time vision of welding pool was captured and displayed as an assistant tool based on a CCD camera (DH-SV1420FM) and a filter-mirror system every 30 s. Table 1 has listed all the welding parameters

During the welding process with consistent energy input, the different degree of penetration would naturally occur due to the influence of heat accumulation if control method is not involved. Besides, the size and shape of welding plates which significantly affects the heat dissipation can result in the change of seam penetration as well. By taking full advantage of these characters, gradient shape of plates was designed to produce various seam penetration, especially under penetration and over penetration, and Y-type groove was also premade for the butt joint welding. As shown in Fig. 2, the necking of the plate is produced to simulate the real faulty welding condition, here it's various heat dissipation caused by the different size of plate width. The measurement signal might not respond this as well as for thickness variation condition, but the subtle change of welding plate is better to check the sensitivity of the extracted sensor features. Furthermore, at the end, different sensory data will be carefully analyzed in order to correlate the feature parameters and the designed disturbance, and then evaluate the welding penetration based on proposed modeling method.

Method and results

Feature extraction of multi-sensor signals

Since these three signals are heterogeneous type of signal, in this paper, different approaches were utilized to extract feature parameters from different signals. Partial signals of interest were selected before the feature extraction.
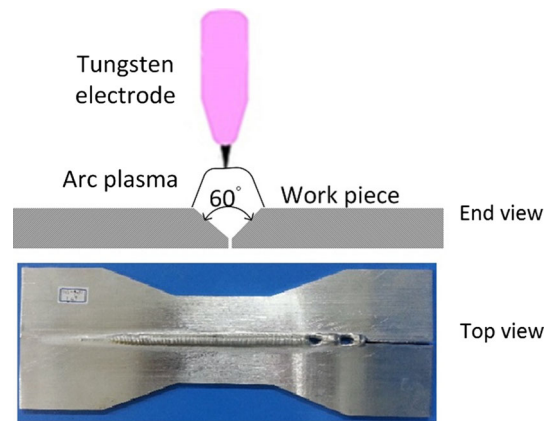

Fig. 2 Schematic of welding disturbance designing

Sound signal

As the left figure shown in Fig. 3, the acquired sound signal would periodically change from peak level to base level due to the character of heat input in pulsed GTAW, which will be found in arc voltage signal in "Voltage signal" section as well. In this paper, the peak signal will be reserved for further real-time processing while the base level signal is discarded for two main reasons, firstly, the base welding current partially has the function of maintaining the welding arc and cathode cleaning; secondly, skipping over from base level has the advantage of having more time to process the signal more accurately and a quicker response in real time processing. After cutting out the peak-level sound signal, certain number of data need to be bundled into a data block before further analyzing and feature extraction in order to meets the requirement of real-time processing speed and accuracy. By careful comparison, the size of the data block is chose to be 3,000 points which corresponds to the seam length of 0.426 mm. The right figure in Fig. 3 also shows one data block of 3,000 points for simultaneously acquired sound signal and voltage signal. It can be seen that there is a peak in every pulse ring down of sound signal which occurs every time the voltage changes, namely, re-arcing in AC pulsed GTAW, which results in the vibration of the welding pool, then, it quickly decreased while the arc gradually turned into stable.

Frequency-domain analysis would be more suitable for sound signal considering its multiple spectrum character. Wavelet packets permits a time-frequency decomposition of the input signal, more importantly, provides a computationally-efficient alternative with sufficient frequency resolution comparing with discrete wavelet transform, because in the WPD, both the detail and approximation coefficients are decomposed to create the full binary tree, for instance, for n levels of decomposition the WPD produces 2^n different sets of coefficients (or nodes) . These wavelet coefficients provide full information in a simple way and a
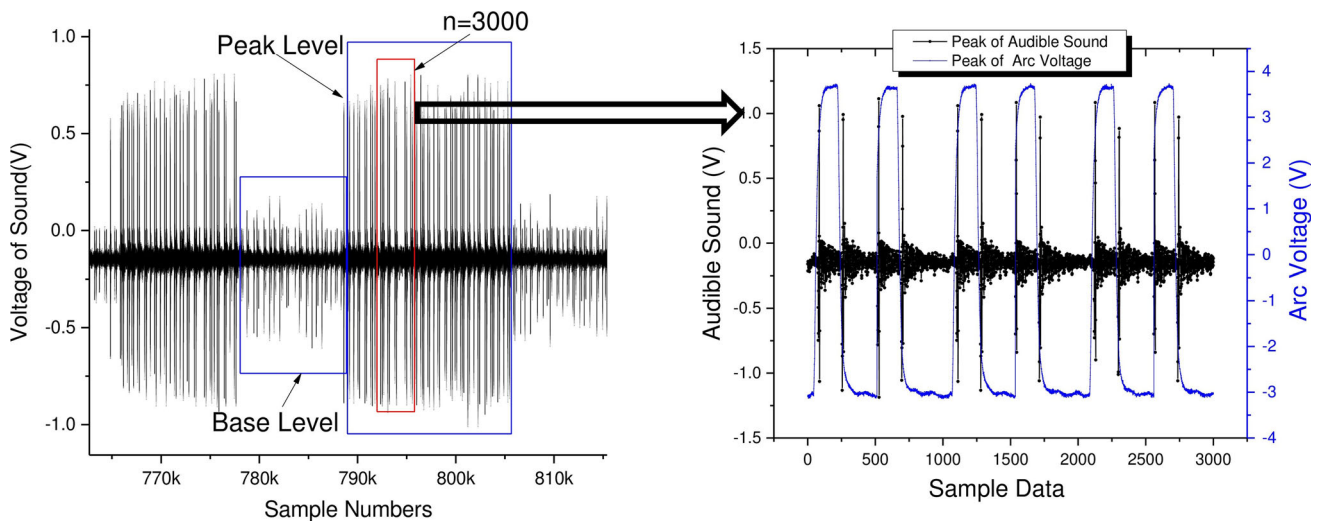
Fig. 3 Acquired sound signal and voltage signal in one data block

Table 2 Statistic parameters of E1–E8 for three type of seam penetration

RMS	E1 (0–1.25 KHz)	E2 (1.25–2.5 KHz)	E3 (2.5–3.75 KHz)	E4 (3.75–5 KHz)
Under penetration	0.772395	0.024598	0.060163	0.042396
Full penetration	0.640746	0.044526	0.086515	0.087697
Burn trough	0.843338	0.02709	0.030917	0.038906
Standard deviation	**0.102801**	0.010858	**0.027812**	**0.027218**
RMS	E5 (5–6.25 KHz)	E6 (6.25–7.5 KHz)	E7 (7.5–8.75 KHz)	E8 (8.75–10 KHz)
Under penetration	0.006105	0.007775	0.056364	0.017851
Full penetration	0.005241	0.016477	0.067575	0.03494
Burn trough	0.004314	0.011478	0.021928	0.012498
Standard deviation	0.000896	0.004367	**0.023788**	0.011721

Higher SD for selected arc sound feature parameters are given in bold

direct estimation of local energies at different scales. Thus, with the use of WPD, a better frequency resolution can be obtained for the decomposed signal. In this paper, relative wavelet energy was calculated based on the square of wavelet coefficient for each frequency band. Specifically, the wavelet coefficients can be obtained as

$$C_j(k) = \langle S, \psi_{j,k} \rangle, \tag{1}$$

where $\psi_{j,k}$ is the orthonormal wavelet function, then, the energy at each resolution level $j = 1,\ldots,-N$, will be the energy of the detail signal

$$EW_j = \sum_k |C_j(k)|^2 \tag{2}$$

In consequence, the total energy can be obtained by

$$Ew_{tot} = \|S\|^2 = \sum_{j<0} \sum_k |C_j(k)|^2 = \sum_{j<0} E_j \tag{3}$$

Then, the normalized values, which represent the relative wavelet energy,

$$E_j = \frac{EW_j}{Ew_{tot}} \tag{4}$$

In this paper, daubechies 3 (db3) was used for wavelet function and the decomposition level is 3. The whole frequency band will be split into 8 sets. For each data block of sound signal, there will be 8, e.g., E1, E2…E8 relative wavelet energy to describe the penetration status of the seam segment as shown in Table 2.

To study the relationship between each frequency level of relative energy and different seam penetration, statistic parameter, firstly, root mean square (RMS) of E1–E8, was calculated for 50 sample data blocks of under penetration, full penetration and burn through respectively. Then, the standard deviation of different penetration status for each wavelet energy was calculated respectively in order to evaluate the performance of each wavelet energy in terms of separating different penetration status. The bigger the STD is, the more
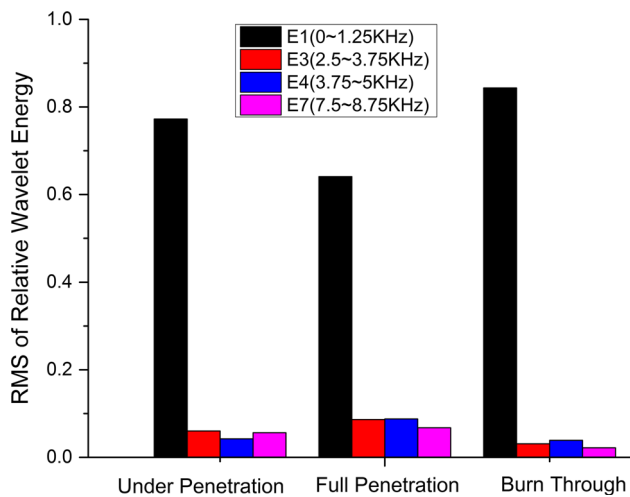
Fig. 4 RMS of relative wavelet energy for different penetration status

Fig. 5 Relative wavelet energy curve of sound for E1, E3, E4 and E7

fluctuation between these three types of penetration is, the more the distance between them is. Table 2 displayed the calculated statistic parameters of E1–E8 for three type of seam penetration, wherein E1 shows the biggest STD with the value of 0.102801, then E3, E4 and E7, which indicates that these four parameters have the better capability of separating different types of penetration status.

Furthermore, the bar chart in Fig. 4 has displayed more about RMS relative wavetlet energy of E1, E3, E4, E7 for different penetration status. On one hand, the wavelet energy in E1, low frequency is much bigger than other frequency bands indicating that the frequency energy of sound signal is mainly distributed in low frequency, on the other hand; E1 for full penetration is the lowest among the three type of penetrations while E3, E4 and E7 for full penetration is higher than others. Figure 5 shows the corresponding feature curves for E1, E3, E4 and E7 that have been filtered using different and suitable method. It is interesting finding in Fig. 5 that the curves of E3 and E7 have the similar shape, which, moreover, displays the opposite character with E1. Specifically, the place where a volley occurs in E1 is a spike in E3 and E7, besides, the dramatic rise at the end of E1 is corresponding to the descending in E3 and E7, which probably can be attributed to the principle of conservation of wavelet energy for sound signal in frequency domain.

Voltage signal

The voltage signal was preprocessed by using the same method with sound signal before feature extraction, including acquiring of signals in peak level and bundling 3,000 of sample data as one data block, which have been both explained in above section . Figure 6 displays the acquired voltage signal which consists of peak level and base level and its one data block for normal and defect welding situation,
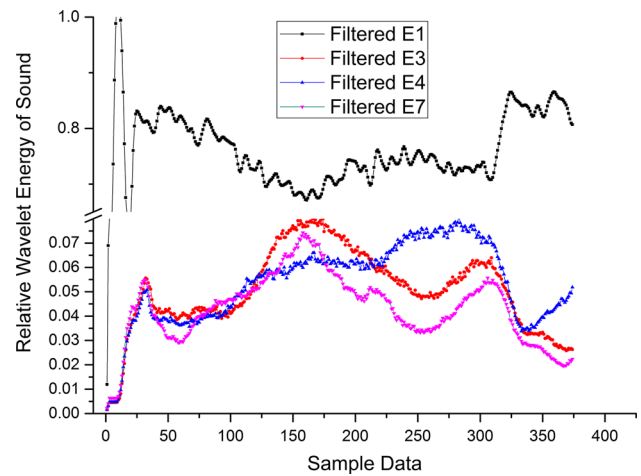
in which shielding gas was largely reduced. It can be seen that the alternative wave of positive and negative was broken, instead, showing mostly positive wave. Figure 7 has shown the flow chart of the feature extraction process for voltage signal. The voltage signal in positive and negative half wave were extracted respectively considering each has the different physical effect on the welding pool based on different threshold value before calculating their statistic parameter as the feature. It is worth to be mentioned that filtering and denoising of the original signal before the feature extraction is extremely necessary based on our current work. In this paper, the moving smooth filter algorithm is applied on the original signal in each data block before feature extraction with the half width of 10 points. RMS is a general parameter used in the monitoring issues, and can estimate relative energy of the voltage signal, and the energy transferred from the welding electrode to the base metal by the electric arc. Figure 8 demonstrates the extracted positive and negative half wave of voltage in one data block, and their corresponding feature curves as well.

Spectrum signal

Spectrum signal, a quite promising sensory tool, has the ability of capturing the intensity of chemical elements appearing in the arc atmosphere. During the GTAW process, most of the elements will be argon atom (ArI) coming from argon shielding gas as well as small proportion of metal elements, such as Al, Mg and so on, which depends on the composition of welding plate and feed wire. In this paper, these two kinds of spectrum emission were carefully analyzed, some of which have been selected to extract feature parameters related to seam penetration. Figure 9 has displayed the acquired spectrum signal during dynamic normal and defect welding process respectively in which some emission
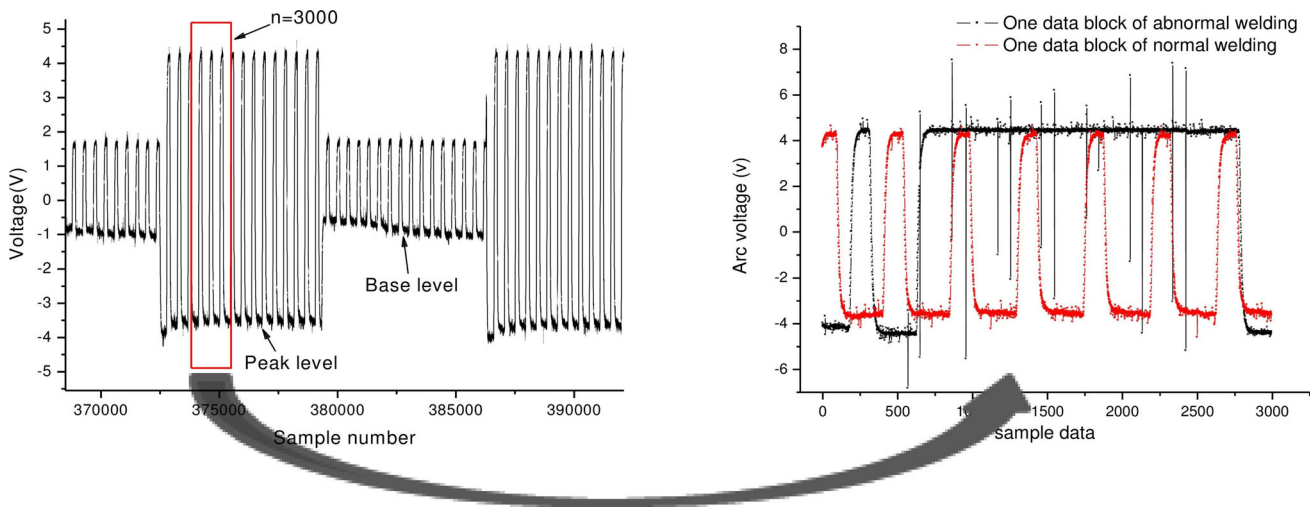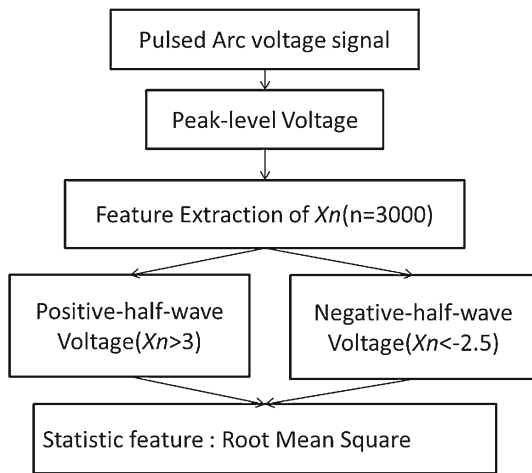
Fig. 6 Preprocessing of voltage signal

Fig. 7 Diagram of feature extraction for voltage signal

lines and selected lines were also marked. It can be seen that when the designed disturbance happened, the intensity of most spectrum lines were much higher than normal welding condition. In addition, most of the spectrum emission lines of metal, such as Al II, Al I, MgI and so on, were distributed in the ultraviolet area and visible area while the emission line of Argon atom can be found in infrared district. Based on the result of Principal Component Analysis (Yu et al. 2013), the emission line of Ar I with the wavelength of 852.14 nm was selected as the first component, from which the spectrum feature was calculated and extracted for this paper's purpose. The other spectrum feature was extracted from the metal zone from 320.24 to 440.75 nm as shown in Fig. 9. Statistic parameters can be an estimation of the spectrum energy of certain element during the welding process. In this paper, RMS of selected metal zone and variance of selected
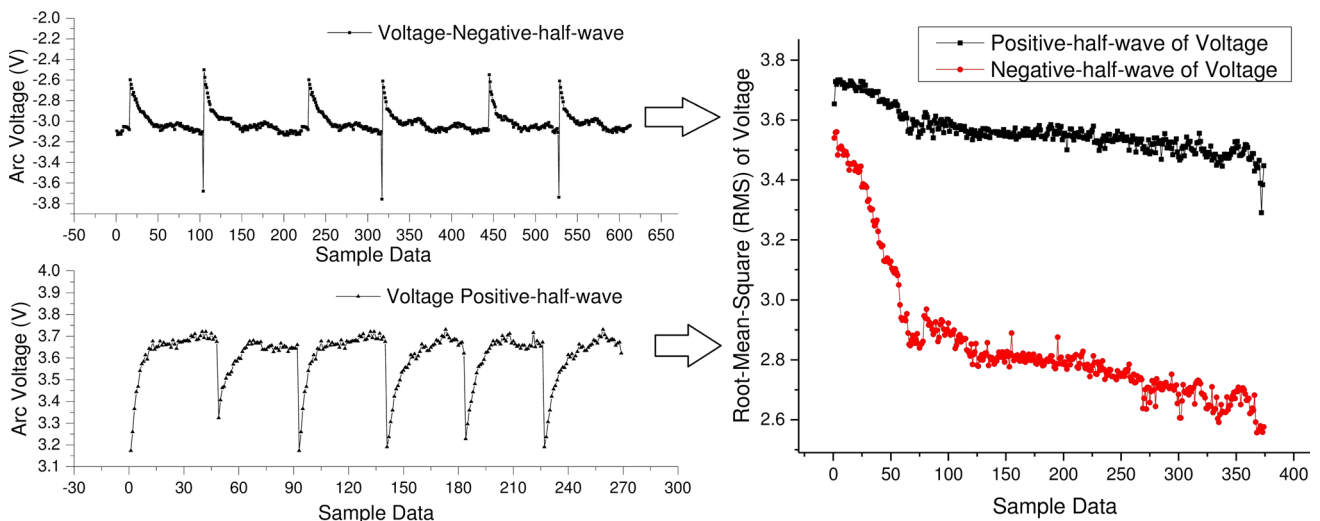

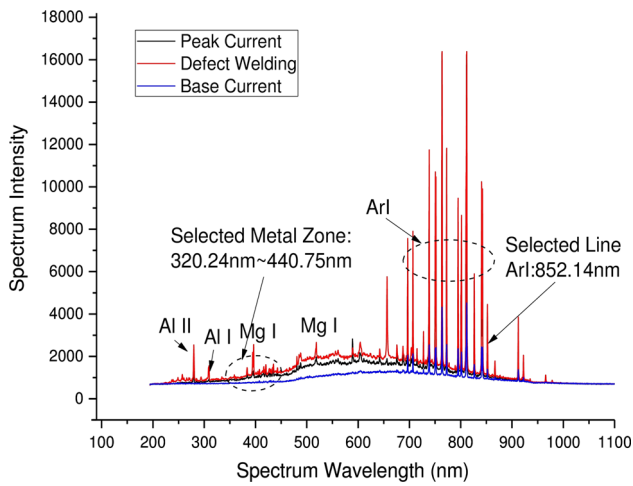**Fig. 8** Feature extraction in time domain for voltage signal

Fig. 9 Acquired spectrum signal in different welding situation

ArI emission line were calculated as feature parameters to indirectly evaluate the stability of welding process and seam penetration. Furthermore, it is quite important to mention that the pulse interference caused by pulsed input energy need to be eliminated by reserving peak-level features and discarding base-level ones because it has to be in consistent with the other two signal features regarding the physical meaning and simultaneous describing of seam penetration. Figure 10 has displayed the original feature curve extracted from ArI emission line and its feature curve on pea-level which, then, was denoised using low pass filtered method. From the left figure, it can be seen that the feature curve shows little change on base-level. The features on peak-level were extracted based on presetting threshold value. A low-pass filter with the cut-off frequency of 0.2Hz was utilized to pass low-frequency signals and attenuates signals with frequencies higher than

the cutoff frequency. Figure 11 also showed the other spectrum feature curves extracted from metal emission zone. In comparison with Fig. 10, it displays more noise and fluctuation implying that the emission of selected metal zone was less stable than that of ArI emission line.

Synchronization of heterogeneous feature data

The key problem when using multisensory data fusion is the synchronization of different type of sensor data. Specifically, the same amount of feature data extracted from each type of sensor is needed to describe the same situation, in this paper, e.g., the penetration status of a whole seam. In other words, each set of multi-feature data should describe the each status of seam penetration at the same place, and then give a more comprehensive estimation than single sensor. As mentioned above, the sound, voltage and spectrum signal have the different sample rate and also diverse feature method have been applied on these signals, which ultimately contributes to the non-uniform feature curves.

In this paper, the method of up sampling was proposed and utilized in the feature curve which has the lower total number of feature data to address this problem. The feature number for sound and voltage signal is both 355 while that for spectrum signal varies with feature due to the different threshold for peak extraction, but they were both lower than 355. So, the feature curves of spectrum signal were up sampled to 355 by means of interpolation by an integer factor. Figure 12 has showed the simultaneous features extracted from sound, voltage and spectrum signals respectively, which are relative wavelet energy E1 of sound, RMS of negative-half-wave—voltage and variance of Ar I emission line, wherein three different penetration status were also marked in the corre-
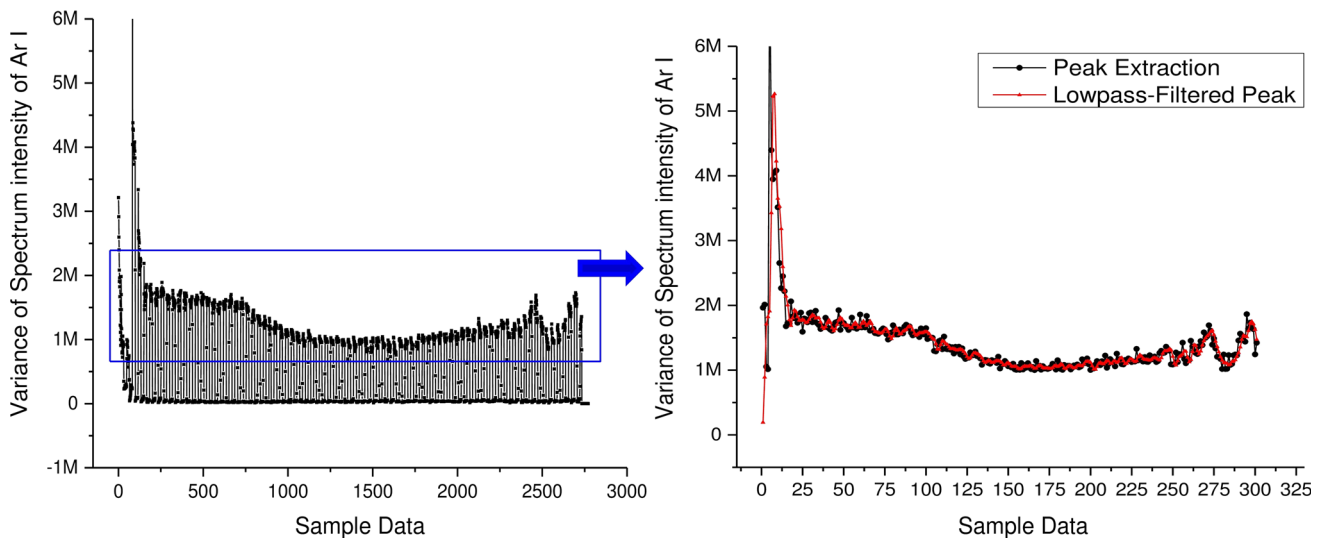

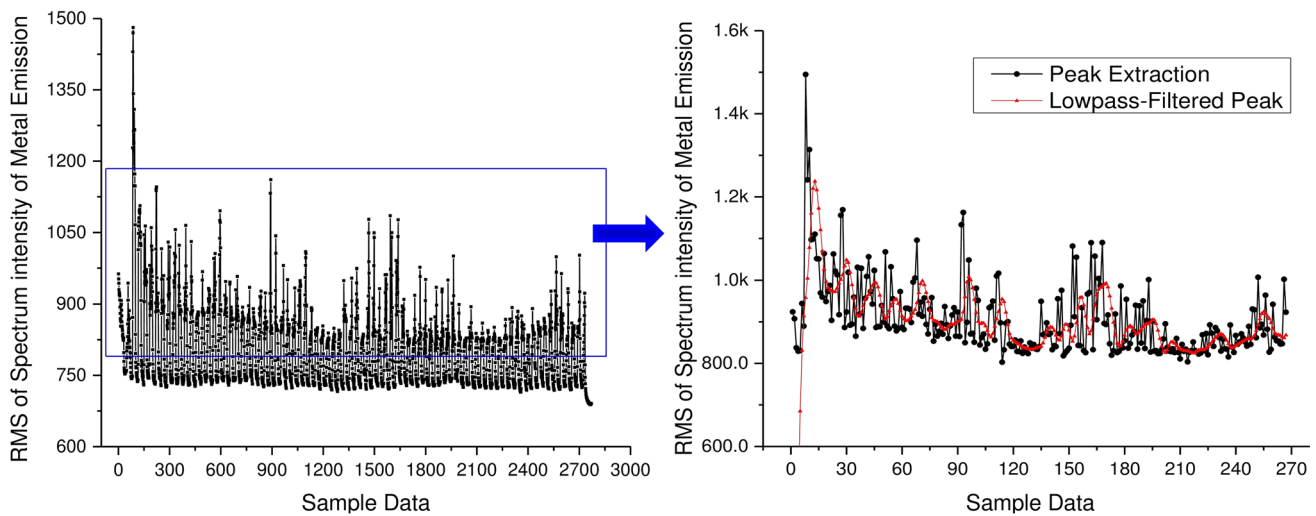**Fig. 10** Feature curve and peak extraction of Ar I emission line

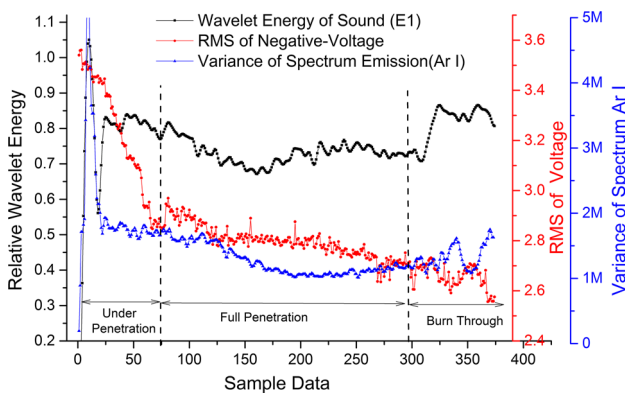**Fig. 11** Feature curve and peak extraction of metal emission

Fig. 12 Simultaneous features of sound, voltage and spectrum signals

Fig. 13 Welded plate with multiple penetration status

sponding place shown in Fig. 13. Under penetration, judging from Fig. 13 has narrower seam width in the front seam while barely shows penetration in the back seam due to insufficient heat energy input, then, the width of plate descends producing satisfied penetration before burning through occurs caused by over heat and bigger gap. From Fig. 12, it can be seen that these three features have demonstrated various degree of sensitivity to seam quality. Specifically, the feature of sound is able to separate the three types of seam penetration quite easily while the other two features were less separable especially regarding the defect of burning-through. However, it is very hard to identify which variable results in such penetration situation. In some cases, different defects display the similar feature in the same monitoring curve. Hence, it is quite necessary to fuse multiple sensor information to establish the unique feature combination for each kind of welding defect. In this case, the various multi-sensory information has demonstrated the absolutely advantage in detecting multiclass of weld defects in addition to the higher classification accuracy over single sensor. The classification performance
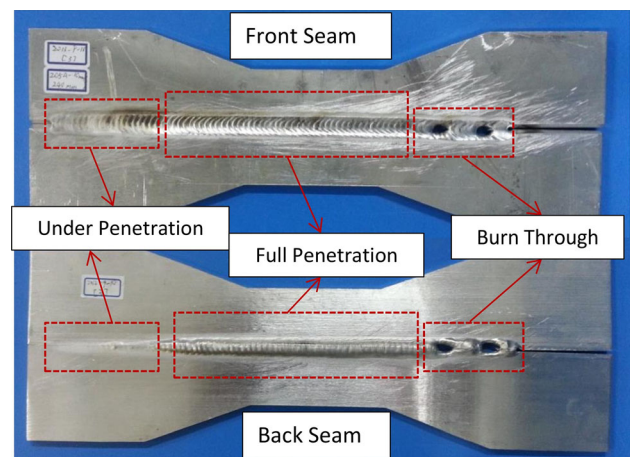
of combined multisensory features was illustrated in Fig. 14, where scatter points with different seam penetration were distributed and well separated by selected multisensory features. Based on the above analyzing, it can be concluded that multisensory data has shown their complementary as well as the redundancy.

Feature-level data fusion based on SVM-CV

Data fusion of arc sound, voltage and spectrum signals in pulsed GTAW seems not very essential considering that pulsed GTAW is quite simple process to produce the good weld quality. However, multisensory technique is still on developing stage regarding this research topic. Quite a few challenges are waiting for being tackled. Applying this technique on GTAW process can give us more time to master the key method for information fusion, which can be possibly
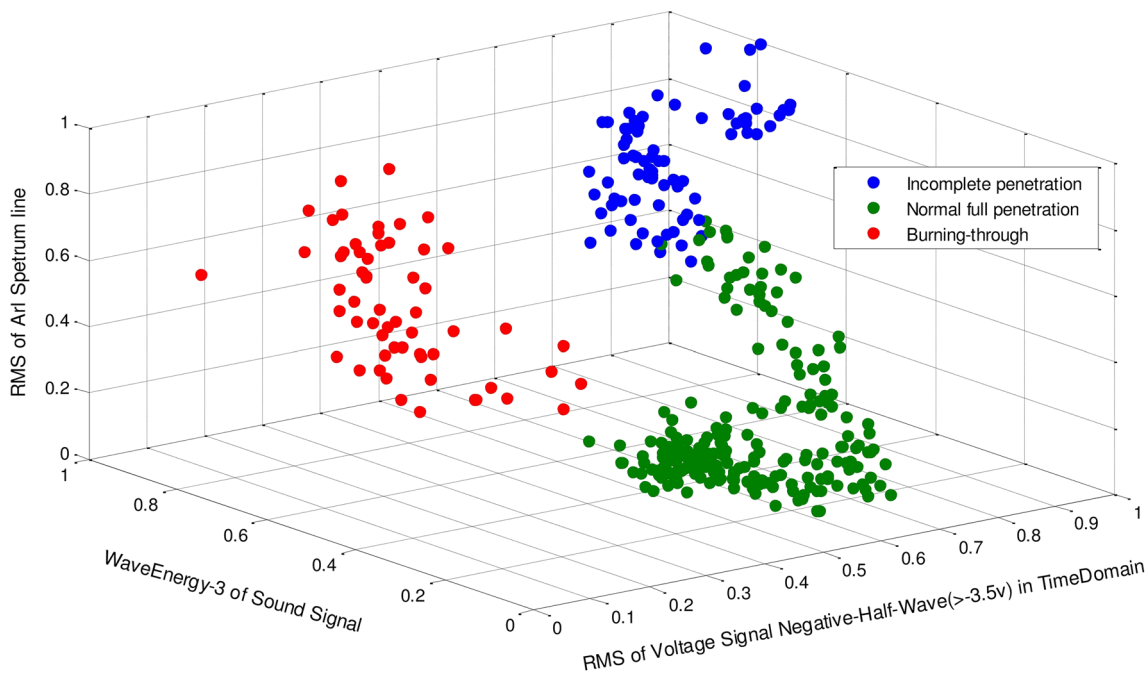
Fig. 14 Scatter distribution of seam samples in 3-D feature space

applied in many other complex and intelligent manufacturing industries. In this section, four classification models were established based on the features of sound, voltage, spectrum and the three sensory fusion respectively to identify the status of each segment of welded seam, and then, compared from the result of mean test accuracy in order to compare and analyze the performance between each single senor and multisensory fusion.

The method of data fusion in this paper was developed based on feature level fusion by normalizing all features extracted from multiple sensors, which also can be considered as a process of heterogeneous-removing, after which it is the same with single sensor modeling. Figure 15 has plotted the flow chart of the proposed feature-level data fusion based on support vector machine and 10-fold cross-validation, namely, SVM-CV classifier, which were illustrated as below. Recent research has indicated the considerable potential of SVM-based approaches for various intelligent classification issues since it is based on the notion that only the training samples that lie on the class boundaries are necessary for discrimination. Consequently, only a small amount of the training samples are actually required but also a high accuracy may be obtained. For multiclass and multifeature problems, it may be extended to allow for nonlinear decision surfaces. In this case, the input data are mapped into a high dimensional space through some nonlinear mapping which has the effect of spreading the distribution of the data points in a way that facilitates the fitting of a linear hyper lane. With this, the classification decision function becomes

$$f(x) = \text{sgn}\left(\sum_{i=1}^{r} \alpha_i y_i k(x, x_i) + b\right) \qquad (5)$$

where α_i, i = 1, ..., r are Lagrange multipliers and $k(x, x_i)$ is a kernel function. The radial basis function(RBF) is chosen as the kernel in this paper,

$$k(x, x_i) = e^{-\gamma \|(x, x_i)\|^2} \qquad (6)$$

where γ and c is the parameter controlling the width of the Gaussian kernel. The accuracy with which a SVM (Foody and Mathur 2004; Frohlich et al. 2003) may classify a data set is dependent on the magnitude of the parameters C and γ. In this paper, cross-validation approach was applied to search the optimal value for these two parameters for the SVM model. Then, the classifier, i.e., SVM-CV was established based on cross-validation while 10-fold cross-validation is used and the mean accuracy for the established prediction model is achieved by calculating the mean value of each fold prediction. In addition, the training and predicting of the SVM-CV was achieved through the combination of Lib-SVM (Chang and Lin 2011) and Matlab.

Table 3 has shown the testing result for these four different classifiers, where each SVM-CV classifier was established based on each single sensor and multisensory fusion respectively. It can be seen that the highest test accuracy was obtained from the multisensory fusion classifier, which was 96.5873 %. This result has well proved that multisensory data has showed its advantage over single sensor. In addition, the SVM-CV classifier based on sound sensor has displayed
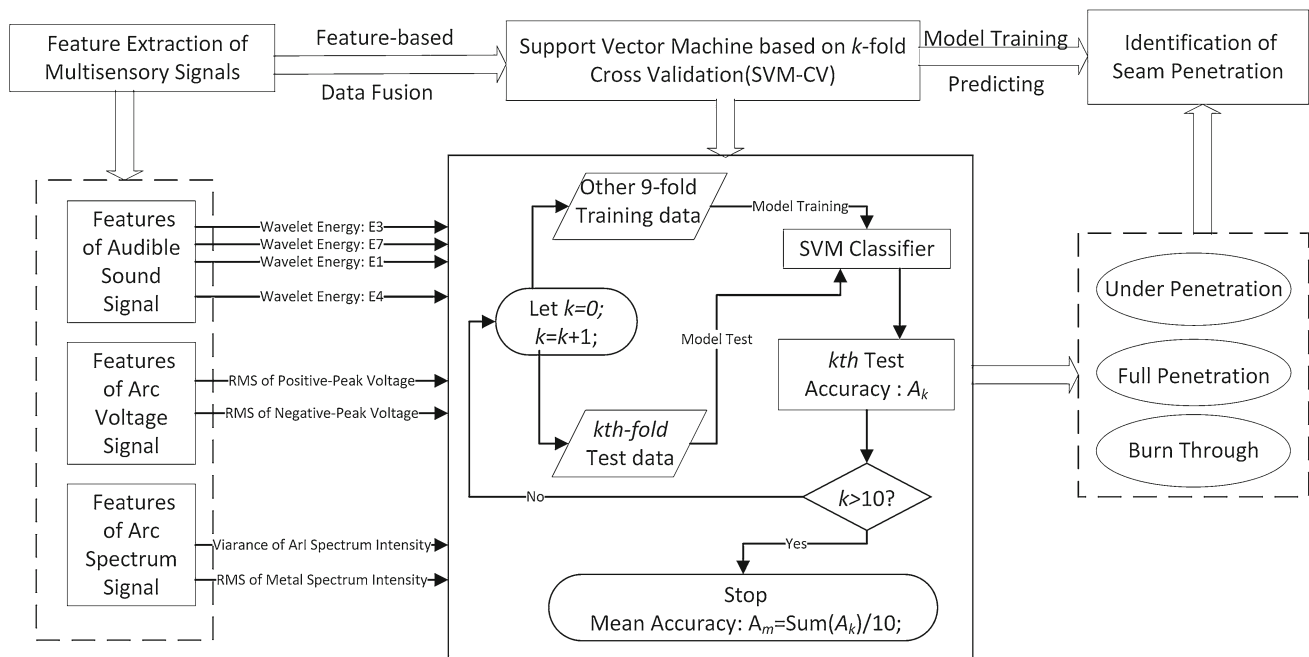
Fig. 15 SVM-CV classifier based on feature-level data fusion

Table 3 Test result for different SVM-CV classifiers

Modeling accuracy	SVM-CV of sound sensor	SVM-CV of voltage sensor	SVM-CV of spectrum sensor	SVM-CV of multi-sensor fusion
Mean test accuracy (%)	92.075	74.0794	77.5079	96.5873

higher accuracy, which was 92.075 %, comparing to the other two single sensor-based classifiers, which indicates that the features extracted from sound signal were more sensitive to the seam penetration than others. This conclusion also shows the agreement with the analyze in "Synchronization of heterogeneous feature data" section. The test accuracy for voltage and spectrum classifier were quite close and relatively lower, e.g., 74.0794 and 77.5079 %.

Discussion

It is worth to mention that the arc sound, voltage and spectrum signals in pulsed GTAW are not quite reliable and dominant signals related to the weld bead quality directly. As some of the other researchers pointed out that it is not the arc itself, but the interaction between the arc and the weld pool which determines the weld quality. Only arc signals are insufficient for monitoring or controlling the weld quality. In addition, the identification of weld defects based on the arc sound, voltage and spectrum signals in pulsed GTAW is still facing some certain difficulty in terms of on line defect detection, then its industrial application potential is limited in certain aspect so far.

Multisensory information fusion

The analysis of frequency energy for arc sound signal in this paper has fair agreement with (Xiao and Den Ouden 1993; Xiao and Ouden 1990; Renwick and Richardson 1983)'s research, wherein the oscillation frequency of welding pool decreased while the welding pool size gradually increased from partially penetration to full penetration. In this paper, the wavelet energy in low frequency (E1) showed the similar feature. However, other frequency energy (E3, E4, E7) all displayed the opposite trend, increasing in full penetration and even burn through condition. The possible reason for this might be that the natural oscillation frequency is in lower frequency which is less than 1 KHz, and higher frequency contains more information about identifying the defect of burning through. In addition, the result from arc voltage signal also showed similar characteristic with the report (Li et al. 2013). As shown in Figs. 8 and 12, the average of arc voltage is smaller for the partial penetration while it became higher for the full penetration, which can be well explained by their proposed dynamic model of welding pool, i.e., thermal expansion and increased total volume of liquid metal along with limited space. In "Synchronization of heterogeneous feature data" section, we presented the method and

result of synchronizing the different kinds of sensor feature parameters trying to identify the welding penetration status. It can be seen that the feature curves of different signals in Fig. 12 showed the corresponding trend along with the dynamic change of welding penetration. However, the partial penetration and burn-through have demonstrated similar range of feature value in sound feature curve, which, in this case, makes it difficult to separate these two types of welding condition, more importantly, multiple defects of weld seam. Hence, it is quite necessary to fuse multiple sensor information to establish the unique feature combination for each kind of welding defect. In this case, the various multisensory information has demonstrated the absolutely advantage in detecting multi-class of weld defects in addition to the higher classification accuracy over single sensor. Moreover, it is quite important to introduce other valuable sensor information of welding process, such as welding pool image, welding current, infrared sensor and so on, to fuse more comprehensive information giving the limitation of each sensor.

Feature selection

A big challenge which we might encounter while using multisensory information fusion is Big Data, which can be quite a burden to the later detection and decision making system. In the part of feature selection for arc sound signal has proposed a simple method of dimension reduction, which can select more sensitive features, such as E1, E3 and so on. It is based on the principle of Fish Distance, which allows the reduced feature space have the smaller inner distance and bigger between distances. More importantly, the optimal feature subset need to be determined in order to obtain as high accuracy for the future classifier as possible. This part of work has been conducted in parallel. The fusion of multi-sensor data in this paper was achieved on feature-based level using SVM-CV classification algorithm. It is also worth to research the decision fusion method, like DS, and other searching method, like SFS, GA, as well as other classification algorithms to be applied on this issue in future.

In the future work, it is worth more time to conduct the correlation analysis between different sensor features. Also, others related to synchronization method of fusing various kind of sensor feature needs to be deeply researched, such as on-line synchronization, fusion speed and resolution loss and so on. Furthermore, more delicate experiment, i.e., different degree of welding defects needs to be carefully designed in order to evaluate the defect not just qualitatively but also quantitatively.

Conclusions

A comprehensive multi-sensor-based method for real-time identification of seam penetration for Al alloy GTAW was developed from signals acquisition, feature extraction and selection to feature-based multisensory data fusion. The main conclusions are as follows:

- Relative wavelet energy of sound signal in specific frequency bands calculated from developed algorithm, namely, E1 (0–1.25 KHz), E3 (2.5–3.75 KHz), E4 (3.75–5 KHz) and E7 (7.5–8.75 KHz) have shown higher sensitivity than others to the status of seam penetration based on the evaluation of feature sensitivity.
- The negative-half-wave of voltage signal has demonstrated more fluctuation than positive-half-wave during the process of designed welding defect.
- The peak-level feature of ArI emission line (852.14 nm) in spectrum signal has displayed higher sensitivity to different welding status while the base-level feature has few changes.
- Multiple status of seam penetration, like incomplete penetration, full penetration and burn through, have been successfully identified by means of the established classification architecture, SVM-CV, while the classifier based on multisensory feature-fusion successfully shows the best performance with the highest test accuracy of 96.5873 %, while the test accuracy for single sound sensor-based classifier is 92.075 % and the lowest is 74.0794 % for voltage sensor.

References

Chang, C.-C., & Lin, C.-J. (2011). LIBSVM: A library for support vector machines. *ACM Transactions on Intelligent Systems and Technology (TIST)*, 2(3), 27.

Chen, S.-B., & Wu, J. (2009). *Intelligentized methodology for arc welding dynamical processes* (Vol. 29). New York: Springer.

Chen, W., & Chin, B. (1990). Monitoring joint penetration using infrared sensing techniques. *Welding Journal*, 69(4), 181s–185s.

Chien, C., & Kannatey-Asibu, E, Jr. (2002). Investigation of monitoring systems for resistance spot welding. *Welding Journal (New York)*, 81(9), 195-S.

Chilian, A., Hirschmuller, H., & Gorner, M. (2011). Multisensor data fusion for robust pose estimation of a six-legged walking robot. In *IEEE/RSJ international conference on intelligent robots and systems (IROS), 2011*, (pp. 2497–2504). IEEE.

Chokkalingham, S., Chandrasekhar, N., & Vasudevan, M. (2012). Predicting the depth of penetration and weld bead width from the infra red thermal image of the weld pool using artificial neural network modeling. *Journal of Intelligent Manufacturing*, 23(5), 1995–2001. doi:10.1007/s10845-011-0526-4.

Christner, B. (1998). Developing a GTAW penetration control system for the Titan IV program. *Welding and metal fabrication*, *66*(3), 29–38.

Cullen, J., Athi, N., Al-Jader, M., Johnson, P., Al-Shamma'a, A., Shaw, A., et al. (2008). Multisensor fusion for on line monitoring of the quality of spot welding in automotive industry. *Measurement*, *41*(4), 412–423.

Emel, E., & Kannatey-Asibu, E. (1988). Tool failure monitoring in turning by pattern recognition analysis of AE signals. *Journal of Eengineering for Industry*, *110*(2), 137–145.

Faouzi, N.-E. E., Leung, H., & Kurian, A. (2011). Data fusion in intelligent transportation systems: Progress and challenges—A survey. *Information Fusion*, *12*(1), 4–10.

Farson, D., & Kim, K. (1999). Generation of optical and acoustic emissions in laser weld plumes. *Journal of Applied Physics*, *85*(3), 1329–1336.

Foody, G. M., & Mathur, A. (2004). Toward intelligent training of supervised image classifications: Directing training data acquisition for SVM classification. *Remote Sensing of Environment*, *93*(1), 107–117.

Frohlich, H., Chapelle, O., & Scholkopf, B. (2003). Feature selection for support vector machines by means of genetic algorithm. In *Proceedings of 15th IEEE international conference on tools with artificial intelligence, 2003* (pp. 142–148). IEEE.

Kannatey-Asibu, E, Jr. (2009). *Principles of laser materials processing* (Vol. 4). London: Wiley.

Lee, S. (2013). *Process and quality characterization for ultrasonic welding of lithium–ion batteries*. Ann Abor: University of Michigan.

Li, P., & Zhang, Y. (2001). Robust sensing of arc length. *IEEE Transactions on Instrumentation and Measurement*, *50*(3), 697–704.

Li, X., Shao, Z., Zhang, Y., & Kvidahl, L. (2013). Monitoring and control of penetration in GTAW and pipe welding. *Welding Journal*, 92, 191–196.

Mirapeix, J., Cobo, A., Conde, O., Jaúregui, C., & López-Higuera, J. (2006). Real-time arc welding defect detection technique by means of plasma spectrum optical analysis. *NDT & E International*, *39*(5), 356–360.

Renwick, R., & Richardson, R. (1983). Experimental investigation of GTA weld pool oscillations. *Welding Journal*, *62*(2), 29.

Smith, D., & Singh, S. (2006). Approaches to multisensor data fusion in target tracking: A survey. *IEEE Transactions on Knowledge and Data Engineering*, *18*(12), 1696–1710.

Sun, A., Kannatey-Asibu, E, Jr, & Gartner, M. (1999). Sensor systems for real-time monitoring of laser weld quality. *Journal of Laser Applications*, *11*(4), 153–168.

Sun, A., Kannatey-Asibu, E, Jr, & Gartner, M. (2002). Monitoring of laser weld penetration using sensor fusion. *Journal of Laser Applications*, *14*(2), 114–121.

Wang, X., & Li, R. (2013). Intelligent modelling of back-side weld bead geometry using weld pool surface characteristic parameters. *Journal of Intelligent Manufacturing* 1–13. doi:10.1007/s10845-013-0731-4.

Xiao, Y., & Den Ouden, G. (1990). A study of GTA weld pool oscillation. *Welding Journal*, *69*(8), 289.

Xiao, Y., & Den Ouden, G. (1993). Weld pool oscillation during GTA welding of mild steel. *Welding Journal (New York)*, *72*, 428-s.

Yu, H., Xu, Y., Lv, N., Chen, H., & Chen, S. (2013). Arc spectral processing technique with its application to wire feed monitoring in Al–Mg alloy pulsed gas tungsten arc welding. *Journal of Materials Processing Technology*, *213*(5), 707–716.

Zhang, W., Liu, Y., Wang, X., & Zhang, Y. (2012). Characterization of three-dimensional weld pool surface in GTAW. *Welding Journal*, *91*(7), 195s–203s.

Zhang, W., Zhang, X., & Zhang, Y. (2013). Robust pattern recognition for measurement of three dimensional weld pool surface in GTAW. *Journal of Intelligent Manufacturing* 1–18. doi:10.1007/s10845-013-0825-z.

Zhang, Y., Wu, L., Walcott, B., & Chen, D. (1993). Determining joint penetration in GTAW with vision sensing of weld face geometry. *Welding Journal (New York)*, *72*, 463-s.

Zhang, Z., Yu, H., Lv, N., & Chen, S. (2013). Real-time defect detection in pulsed GTAW of Al alloys through on-line spectroscopy. *Journal of Materials Processing Technology*, *213*(7), 1146–1156.